Miner Deposita (2006) 41:771–783
DOI 10.1007/s00126-006-0094-2

ARTICLE

Genesis of the Permian Baimazhai magmatic Ni–Cu–(PGE) sulfide deposit, Yunnan, SW China

Christina Yan Wang · Mei-Fu Zhou

Received: 22 May 2006 / Accepted: 23 August 2006 / Published online: 3 October 2006

Abstract The ~260 Ma-old Baimazhai Ni–Cu–(PGE) sulfide deposit in the Jinping region, Yunnan, SW China, is hosted in a small mafic–ultramafic intrusion, which intruded Ordovician sandstone and slate. The intrusion is concentric with lens shape, about 530 m long, 190 m wide and 24 to 64 m thick, trends 296°, and dips 22°NE. The massive sulfide ore body forms the core of the intrusion and is surrounded by variably mineralized orthopyroxenite, websterite and barren gabbro. The proportion of gabbro, websterite, orthopyroxenite and massive ore is approximately 30, 30, 20 and 20 vol.%, respectively. Magmatic pyrrhotite, pentlandite and chalcopyrite make up more than 90% of the massive ores. The massive ores contain high Ni (1.6 to 4.2 wt%) and Cu (0.4 to 6.5 wt%) and low ∑PGE contents (85 to 524 ppb). They have Pd/Ir ratios ranging from 6.7 to 530, Pd/Pt ratios from 0.7 to 2.6 and Cu/(Pd×1,000) ratios from 31 to 400, which are comparable with those of the silicate rocks [Pd/Ir=4 to 183, Pd/Pt=0.7 to 3.5, and Cu/(Pd×1,000)=100 to 400]. Similar Pd/Pt and Cu/Pd ratios of the silicate rocks and massive ores throughout the intrusion indicate a single sulfide segregation event. Excess sulfide melt segregation resulted from intensive crustal contamination that formed Si-rich and Mg-rich basaltic magmas in a deep-seated staging chamber before magma emplacement. The immiscible sulfide melts and the silicate melts were eventually evacuated from the staging magma chamber by compressive forces. Flow differentiation under high velocity concentrated the sulfide melts toward the middle of the magma flow, and consequently, formed a massive sulfide ore body in the central part of the intrusion. Low concentrations of PGEs and general absence of platinum-group minerals in the massive ores may have resulted from a relatively large mass fraction of the sulfide melts (e.g. *R*-factor=~70) in Baimazhai compared with other intrusions elsewhere, such as Noril'sk-Talnakh with a *R*-factor of >10,000.

Keywords Nickel sulfide mineralization · Platinum-group elements · Sulfur saturation · Baimazhai · China

Introduction

Economically important magmatic Ni–Cu–(PGE) sulfide deposits occur in dynamic environments such as magma conduits and lava channels. The enhanced ore potential of conduit systems is attributed to their specific flow environment and to the exploitation of the conduits by multiple magma flows (Maier et al. 2001). Such environments were documented at Kambalda in Western Australia (Lesher and Keays 2002), Noril'sk in Russia (Naldrett et al. 1996; Lightfoot and Keays 2005), the Uitkomst deposit associated with the Bushveld Complex in South Africa (Gauert et al. 1995), the Voisey's Bay intrusion associated with the Nain Plutonic Suite in Canada (Lightfoot and Naldrett 1999). In these localities, sulfides entrained and transported by ascending silicate magmas were concentrated in the widened parts of the conduits or near their exits into larger chambers, owing to a decrease in the flow velocity. The precipitated sulfides were further upgraded by reaction with continued surges of undepleted magma using the same

Editorial handling: P. Lightfoot

C. Y. Wang (✉) · M.-F. Zhou
Department of Earth Sciences, The University of Hong Kong, Hong Kong, China
e-mail: wangyan2002@hkusua.hku.hk

conduit. Thus, the sulfide deposits are commonly located at the base or margin of mafic–ultramafic intrusions or lava flows.

Many small, mineralized mafic–ultramafic intrusions in China have large proportions of sulfides relative to the volume of silicate rocks (Tang 1993; Zhou et al. 2002a). For example, over 43 vol.% of the Jinchuan intrusion in NW China and over 90 vol.% of the No. 7 intrusion in Hongqiling in NE China are mineralized with disseminated or massive Ni–Cu–(PGE) sulfides (Tang 1993; Tang and Li 1995; Zhou et al. 2002a). In these two examples, the sulfides are centrally disposed within the intrusions. The Jinchuan intrusion is thought to have formed from multiple injections of compositionally different magmas, whereas the massive sulfide bodies are considered to be the last injection of sulfide melts (Tang 1993; Tang and Li 1995; Song et al. 2006). However, de Waal et al. (2004) explained the formation of the intrusion as the result of injection of a viscous crystal mush containing variable amounts of sulfide liquid and silicate melt of high-Mg basaltic composition into planar fractures or faults.

Like the Jinchuan and Hongqiling intrusions, the Permian Baimazhai intrusion in the Jinping region, SW China, is also a concentric body with a centrally disposed massive sulfide ore body surrounded by orthopyroxenite, websterite and gabbro (Wang et al. 2006). A large proportion (~70 vol.%) of the intrusion is mineralized. The Ni grades of ores range from 0.17 to 4.5 wt% with an average grade of 1.03 wt% and Cu grades from 0.12 to 2.3 wt% with an average of 0.81 wt% (unpublished data of the Jinping Nickel Mine). The estimated reserve of Ni metal is 50,000 tonnes with Ni from the massive ores making up ~60% of the reserve, according to an exploration project by a local geological team in the 1960s (unpublished data of the Jinping Nickel Mine). The deposit is currently being mined. Thus, the Baimazhai intrusion provides an opportunity to develop and evaluate genetic models that explain the formation of large volumes of sulfides in very small intrusions.

The geochemistry of the silicate rocks of the Baimazhai intrusion indicates that they formed from siliceous, high-magnesium basaltic magmas with extensive crustal contamination (~35%) from low-Ti picritic parental magmas (Wang et al. 2006). The chalcophile metals are shown to be extremely useful for unraveling the S-saturation history of the magmas. In this paper, we describe the massive ores and present new Ni, Cu and PGE analyses. The data are compared and contrasted with data for the silicate rocks. Our main objective is to better understand the magmatic evolution and S-saturation history of the Baimazhai deposit to develop a model in which large volumes of sulfide melt can be concentrated in small intrusions.

Geological background

Southwest China consists of the Yangtze Block to the east and the Tibetan Plateau to the west. The Yangtze Block is composed of a crystalline basement known as the Kangding Complex (Neoproterozoic) (YBGMR 1990) overlain by a thick sequence of Sinian to Mesozoic strata of shallow marine origin. Permian strata include carbonate-rich rocks and the Emeishan continental flood basalts. Triassic strata include both continental and marine sedimentary rocks, whereas Jurassic to Cretaceous strata are entirely continental. All these rocks were deformed by a late Mesozoic northwest directed overthrust system (Yan et al. 2003).

The Emeishan large igneous province (ELIP) is exposed over a large part of SW China and northern Vietnam and is composed of flood basalts, and spatially and temporally associated mafic–ultramafic intrusions. The flood basalts cover an area of more than 5×10^5 km^2 with thicknesses ranging from several hundred meters up to 5 km (Chung and Jahn 1995; Song et al. 2001; Xu et al. 2001) (Fig. 1a). In the Jinping region, the flood basalts lie south of the Ailao Shan–Red River (ASRR) fault zone and belong to the southernmost part of the ELIP. The flood basalts in Jinping, up to 4.5 km in thickness (YBGMR 1990), lie between the early Permian Yangxin Formation and the Triassic Gejiu Formation. The basaltic sequence consists mainly of massive aphyric or weakly plagioclase-phyric lavas with lesser amounts of interlayered volcanic breccia and tuff.

In the Baimazhai–Yingpanjie area, Ordovician strata are in tectonic contact with the ASRR fault zone, which is composed of Paleoproterozoic schist and gneiss and Proterozoic granite (Fig. 1b). A group of small, differentiated plutons associated with the Emeishan flood basalts intrude Ordovician meta-sandstone and slate (Fig. 1b). One of these, the Baimazhai mafic–ultramafic intrusion, hosts a Ni–Cu–(PGE) sulfide ore deposit. The intrusion is lens-shaped, about 530 m long, 190 m wide and 24 to 64 m thick, and trends 296° and dips 22°NE (Fig. 4–11 of Tang et al. 1989; Fig. 4 of Zhang et al. 2006). The intrusion crops out in an area of 0.1 km^2 on the surface with its major part unexposed. The intrusion itself is cut by Cenozoic lamprophyre dykes (Guan et al. 2003).

The intrusion is a concentric body composed of an inner core of massive sulfide ore surrounded by orthopyroxenite, websterite and gabbro (Fig. 1c). Both orthopyroxenite and websterite are variably mineralized, and have net-textured ore and disseminated ore, respectively. The gabbro is generally sulfide-free. The massive ore body in the central part of the intrusion is about 425 m long, 40 to 72 m wide, and 0.7 to 21 m thick, as demonstrated by an extensive drill and exploration program conducted by local geological teams. The proportion of gabbro, websterite, orthopyroxenite

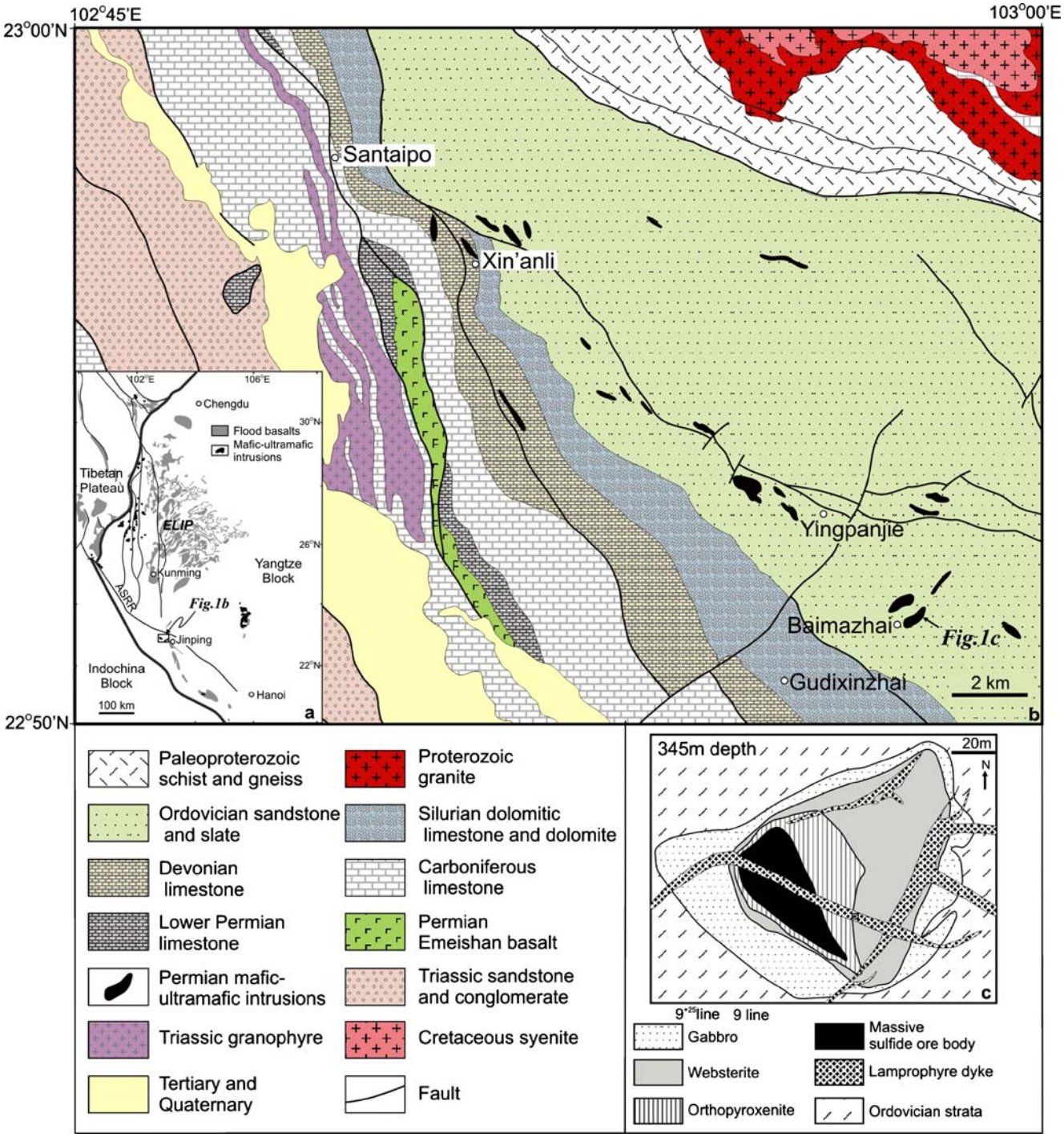

Fig. 1 (**a**) Simplified geological map showing the occurrence of the Emeishan large igneous province (ELIP) in SW China and northern Vietnam and the tectonic location of the Baimazhai Ni–Cu–(PGE) sulfide deposit (modified from Song et al. 2001; Zhou et al. 2002b and the geological map of Vietnam). (**b**) Simplified geological map showing the distribution of the Permian Emeishan flood basalts and mafic–ultramafic intrusions in the Baimazhai area (modified after the 1:50,000 geological map of the Gudixizhai section, the Jinping area, Regional Geological Survey Team of the Yunnan Bureau of Geological and Mineral Resource, 2001). (**c**) A planar of the Baimazhai intrusion at 345 m depth, showing the distribution of rock units and massive sulfide ores (after the unpublished data of the Jinping Nickel Mine)

and massive ore in the intrusion is approximately 30, 30, 20 and 20 vol.%, respectively (Fig. 1c).

Petrography and mineralogy

Sulfide ores

Three types of ores were observed in the Baimazhai intrusion; massive, net-textured, and disseminated. The massive ores have sulfides ranging from 52 to 88 wt%, whereas the net-textured ores contain variable amounts of sulfides ranging from 1.2 to 61 wt%. The massive and net-textured ores account for about 90% of the Ni, Cu and PGE reserves of the intrusion, and they generally have sharp contacts with each other (Fig. 2a). The massive ores average about 3.1 wt% Ni, 2.9 wt% Cu and 0.09 wt% Co, whereas the net-textured ores have an average of 1.0 wt% Ni, 0.7 wt% Cu and 0.03 wt% Co. The total PGE contents of the massive ores range from 85 to 524 ppb (Table 1), and the net-textured ores average about 60 ppb (Wang et al. 2006). The disseminated ores contain 0.11 to 17 wt% sulfide.

The massive ores are composed mainly of pyrrhotite (Po) (85%) with fewer pentlandite (Pn) (10%) and chalcopyrite (Cp) (5%) (Fig. 3a). Most of the massive ores have subhedral granular textures. Flame textures resulting from pyrrhotite–pentlandite exsolution and embayed textures formed by replacement processes are also present (Fig. 3a). Granular magnetite (Mt) makes up 2 to 8 vol.% of the massive ores.

In the net-textured ores the sulfides fill interstitial voids in the orthopyroxene (Opx) cumulates (Fig. 2b), and sometimes occur along cracks or cleavage planes in secondary minerals.

In the disseminated ores, the sulfides typically form granular aggregates up to 3.5 mm across, randomly distributed between the silicate grains (Fig. 2c).

In addition to the ores described above, minor brecciated ores locally form thin layers in a thickness ranging from 0.8 to 5 m and occur along the boundary of the intrusion, suggesting some tectonic deformation. The brecciated ores are composed of silicate fragments cemented by sulfides, locally associated with quartz and carbonate. The cementing sulfides consist of the same minerals as the massive ores but have relatively higher contents of chalcopyrite.

Base-metal sulfides (BMS)

Subhedral to anhedral pyrrhotite is coarse-grained (>0.5 mm in diameter) and is commonly associated with pentlandite. Pentlandite occurs as fine-grained inclusions in pyrrhotite, as rims around pyrrhotite grains, as oriented lamellae or as blades along fractures and grain boundaries (Fig. 3b). These textures are similar to those produced experimentally by crystallization of a sulfide melt (Kelly and Vaughan 1983). Chalcopyrite forms anhedral grains of variable size, and in a few cases occurs as veinlets. It typically occurs as aggregates in the interstices between pentlandite, pyrrhotite and magnetite grains and/or replaces

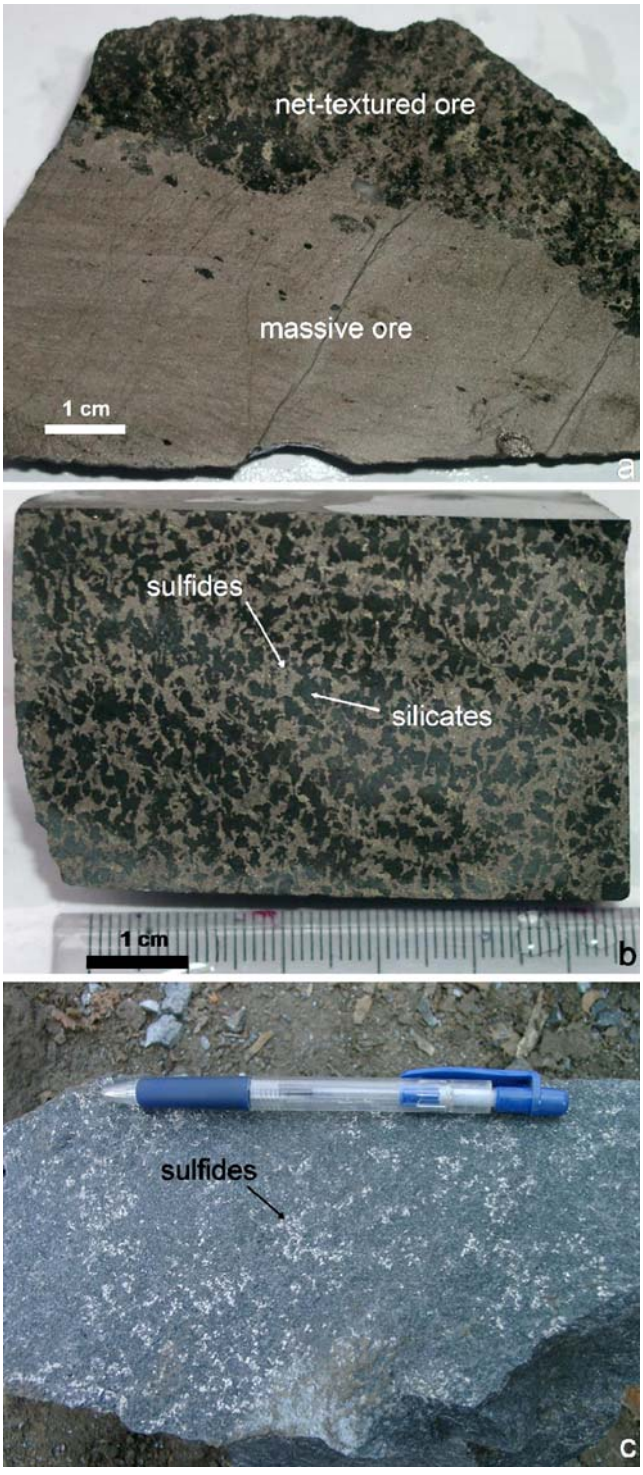

Fig. 2 Three ore types of the Baimazhai deposit. (**a**) Sharp boundary of massive ore and net-textured ore; (**b**) polished drill core sample of net-textured ore; (**c**) disseminated ore

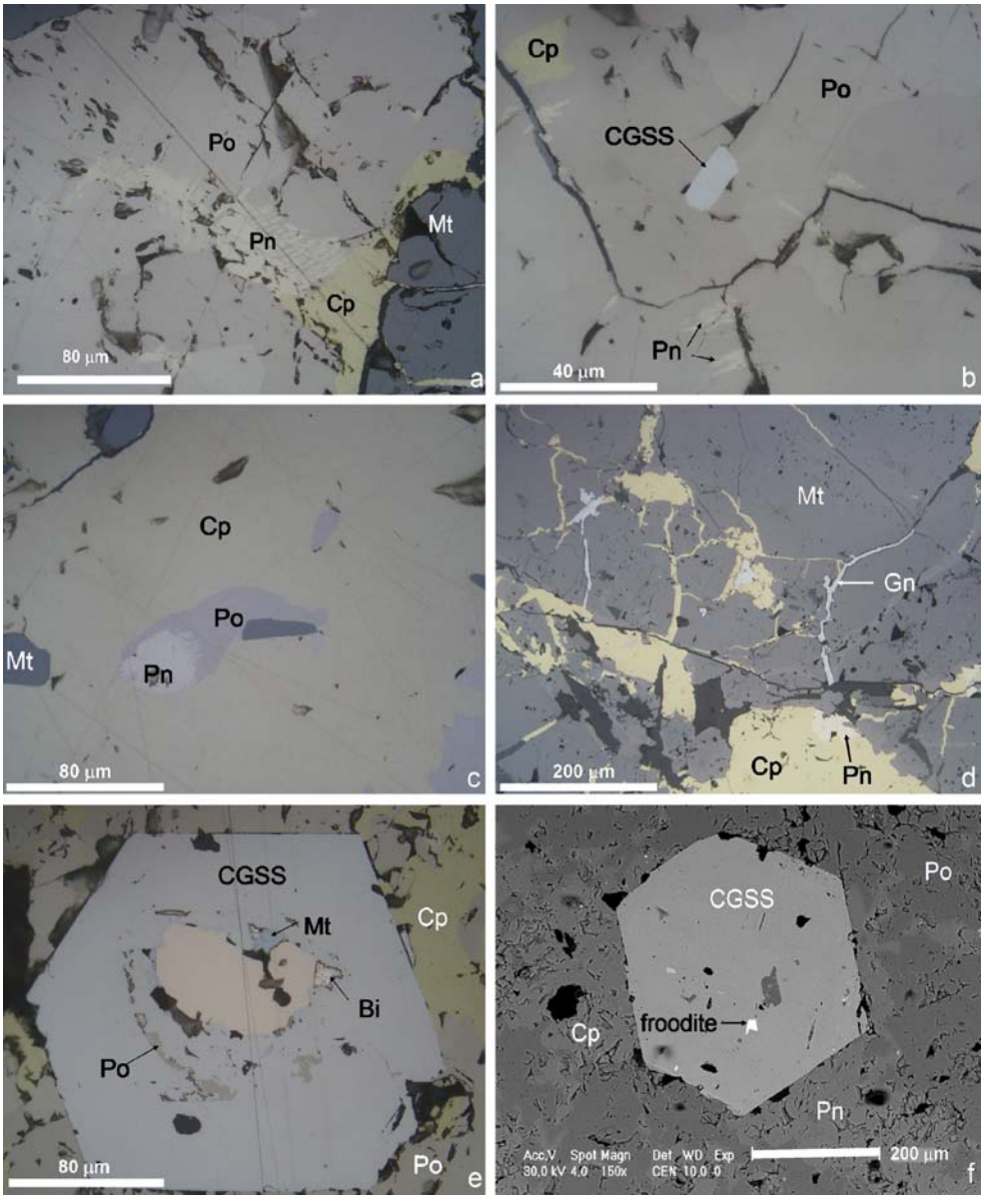

Fig. 3 Microphotos showing ore minerals and textures of the massive ores. (**a**) Primary BMS minerals including pyrrhotite (Po), pentlandite (Pn) and chalcopyrite (Cp) and flame texture, under reflected light; (**b**) flame-like pentlandite occurs along the fractures of pyrrhotite grains, under reflected light; (**c**) pyrrhotite–pentlandite solid solution enclosed within chalcopyrite, under reflected light; (**d**) magnetite (Mt) is crosscut by fractures filled by chalcopyrite and galena (Gn), under reflected light; (**e**) heterogeneous cobaltite–gersdorffite (CGSS) grain varying in composition from gersdorffite (pink color) in the core outwards to cobaltite (gray color), under reflected light; (**f**) froodite enclosed within CGSS, BSE image

them. Patches of fine-grained, granular pyrrhotite–pentlandite solid solution are enclosed within the chalcopyrite (Fig. 3c). Chalcopyrite-filled fractures also cut magnetite grains (Fig. 3d), indicating that the magnetite crystallized before the BMS in the sulfide melts (Prichard et al. 2004). Therefore, the order of crystallization of the ore minerals was Mt→Po+Pn→Cp.

Cobaltite–gersdorffite solid solution (CGSS)

The CGSS crystals are light ivory in color and usually form euhedral to subhedral grains from 10 to 180 μm in diameter. Most CGSS grains are associated with aggregates of pyrrhotite, or accompanied by crystals of pentlandite and chalcopyrite, or even enclosed within chalcopyrite. Some CGSS grains have fractures filled with chalcopyrite, indicating that the CGSS grains formed earlier than chalcopyrite. Some large CGSS grains (>0.1 mm) are zoned from gersdorffite in the core to cobaltite on the rim (Fig. 3e).

Platinum-group minerals (PGM)

In Baimazhai, the massive ores contain very few PGM, consistent with their low PGE contents. One small froodite ($PdBi_2$) grain (~10 μm) was observed within CGSS. The froodite is white with a faint grey tint in reflected plane-polarized light, and is bright white in BSE image (Fig. 3f).

Other ore minerals

Bismuth–tellurium assemblages in the massive ores include bismuthides and tellurides, containing native bismuth

(Fig. 3e), parkerite and hedleyite, and are believed to be related to later hydrothermal alteration. The native bismuth is associated with froodite. Minor galena (Fig. 3f), pyrite, and arsenopyrite are also present and are typically associated with aggregates of pyrrhotite accompanied by chalcopyrite and magnetite.

Analytical methods

Samples were selected from a drill core that penetrated a massive sulfide layer (~16 m in thickness). Major oxides (except SiO_2) and selected trace elements, including V, Cr, Ni and Cu, were obtained using inductively coupled plasma-atomic emission spectroscopy (ICP-AES) at the Guangzhou Institute of Geochemistry, China. The samples were digested with 1 ml of concentrated HF and 0.5 ml of concentrated HNO_3 in screw top PTFE-lined stainless steel bombs at 190°C for 12 h. Lutetium was mixed in the solution as an internal standard. The precision of the analyses was generally better than 1% for concentrations greater than 200 ppm, and 1 to 3% for concentrations less than 200 ppm. International geochemical standards (GSR-1 granite, GSR-3 basalt, GSR-5 shale, RTS-2 and RTS-3 sulfide ores, GBW-07267 pyrite, and GeoPT-12 ultramafic rock) were used for calibration.

Silica and S were obtained using a gravimetric method in the Guangzhou Institute of Geochemistry and the University of Hong Kong, respectively.

REE concentrations were obtained using the pre-concentration method described by Qi et al. (2005). Other trace elements were analyzed following the protocol of Qi et al. (2000) by inductively coupled plasma-mass spectrometry (ICP-MS) at the University of Hong Kong. Pure elemental standards were used for external calibration, and BHVO-1 (basalt) and BCR-1 (basalt) were used as reference materials. The accuracies of the ICP-MS analyses were better than ±10% and precisions normally less than 3%.

The PGE analyses were performed using the ICP-MS at the University of Hong Kong after NiS fire assay and Te-precipitation. The standard reference materials used in the procedure were WMS-1 (a sulfide ore) and WPR-1 (an ultramafic rock). The accuracy of the technique is estimated to be better than ±5% for Rh, Pd and Ir, and 10% for Pt. The procedural blanks were 0.23 ppb Ru, 5.48 ppb Pd, 0.10 ppb Ir, 0.73 ppb Pt and 0.06 ppb Rh.

Analytical results

The major elements, trace elements (including REE and PGEs), S, Cu and Ni of the massive ores are listed in Table 1. The S contents of the massive ores range from 19.1 to 33.6 wt%, corresponding to 51.6 to 88.6 wt% sulfides (Table 1). The massive ores are mainly composed of S, Fe, Cu and Ni with minor Si, Ti, Al, Mn, Mg and K associated with enclosed silicates.

The massive ores contain 1.56 to 4.21 wt% Ni and 0.40 to 6.5 wt% Cu (Table 1). The Ni/Cu ratios range from 0.2 to 7.6 with an average of 1.9. The Cu and Ni contents vary as a function of the S and sulfide contents. The massive ores generally show a trend from Ni-rich to Cu-rich, indicating fractionation of sulfide melt (Fig. 4).

The massive ores have wide ranges of Pd (38 to 313 ppb), Pt (32 to 222 ppb) and Pd/Ir ratios (6.7 to 530), but relatively constant Pd/Pt ratios (0.8 to 2.6). Cu/(Pd×1,000) ratios range from 31 to 400. On the chondrite-normalized chalcophile element diagrams, the massive ores show relatively steep, trough-like patterns (Fig. 5). On the plot of Pd/Ir vs Ni/Cu, the massive ores follow a differentiation trend of sulfide melt from Ni-rich to Cu-rich along the mantle line, and plot in the fields of both layered intrusions and flood basalts (Fig. 6). In the plot of sulfide content vs Cu/Zr ratio (Fig. 7a), the massive ores have higher Cu/Zr (Cu/Zr=8,700 to 133,000) ratios than those of the silicate rocks of the intrusion. The Cu/Zr ratios of the silicate rocks vary positively with the sulfide contents of the rocks. The sulfide-poor gabbros and websterites have Cu/Zr ratios lower than 1 whereas the sulfide-rich orthopyroxenites have Cu/Zr ratios ranging from 3.3 to 2,240 (Fig. 7a). On the plot of Pt/Y vs Pd/Cr, the massive ores have the highest Pd/Cr and Pt/Y ratios, whereas the sulfide-poor gabbros have the lowest Pd/Cr and Pt/Y ratios (Fig. 7b). The Pd/Cr and Pt/Y ratios correlate positively in the silicate rocks and decrease dramatically from the net-textured ores to the sulfide-poor gabbros (Fig. 7b).

Discussion

Magmatic origin and hydrothermal overprinting of the deposit

The Baimazhai sulfide deposit is hosted in a mafic–ultramafic intrusion and has many magmatic features, although these features were later overprinted by strong hydrothermal alteration (Zhang et al. 2006). Tectonic movements may have affected the body somewhat, as indicated by the brecciated sulfide ores along its margins. However, the hydrothermal fluids may not have completely altered the massive sulfide ore body.

The net-textured and disseminated sulfide ores (Fig. 2b, c) show clear evidence of crystallization from the immiscible sulfide melt. In the massive ores, granular pentlandite surrounds pyrrhotite or occurs along fractures within pyrrhotite grains, indicating exsolution of monosulfide

Table 1 Major and trace elements of the massive ores from the Baimazhai deposit

Sample No.	BMZ-90	BMZ-91	BMZ-92	BMZ-93	BMZ-94	BMZ-95	BMZ-96	BMZ-97	BMZ-98	BMZ-99	BMZ-100	BMZ-101	BMZ-102	BMZ-103	BMZ-104	BMZ-105	BMZ-106
Major elements (wt%)																	
SiO_2	0.34	0.36	0.43	0.59	0.37	0.93	0.22	0.64	0.58	0.27	0.16	0.15	0.18	0.21	0.19	0.19	0.14
TiO_2	0.13	0.04	0.01	0.01	0.01	0.01	0.03	0.01	0.01	0.01	0.03	0.02	0.03	0.03	0.03	0.05	0.02
Al_2O_3	0.08	0.03	0.02	0.02	0.02	0.03	0.03	0.03	0.03	0.02	0.03	0.03	0.03	0.03	0.03	0.04	0.03
Fe (total)	53.6	54.2	56.3	56.1	56.7	57.5	54.7	57.5	57.6	54.3	54.0	55.3	54.8	53.8	54.0	54.5	54.0
MgO	0.17	0.06	0.02	0.03	0.03	0.13	0.02	0.06	0.08	0.04	0.03	0.06	0.03	0.04	0.04	0.04	0.04
MnO	0.08	0.04	0.04	0.07	0.05	0.34	0.09	0.18	0.27	0.04	0.06	0.04	0.06	0.04	0.04	0.04	0.02
CaO	0.04	0.02	0.02	0.02	0.01	0.06	0.01	0.02	0.02	0.01	0.01	0.01	0.01	0.02	0.01	0.01	0.01
Na_2O	0.01	0.01	bdl	0.01	0.01	0.02	bdl	bdl	bdl	bdl	bdl	0.01	bdl	bdl	bdl	0.01	0.01
K_2O	0.04	0.04	0.04	0.04	0.04	0.04	0.04	0.04	0.04	0.04	0.04	0.04	0.04	0.04	0.04	0.04	0.04
S	30.55	29.82	26.81	25.1	28.63	20.87	30.24	19.23	19.09	27.47	32.29	31.73	30.86	32.1	30.89	32.16	33.59
Ni	3.28	3.07	2.73	2.56	3.11	1.77	3.27	1.59	1.56	2.81	3.87	3.95	3.82	3.68	3.64	3.76	4.21
Cu	2.37	3.06	3.12	2.72	0.41	4.85	2.28	6.19	6.50	4.87	1.91	0.88	1.76	2.31	2.44	2.26	0.87
Sulfide (wt%)	80.4	78.7	70.8	66.3	74.8	55.8	79.6	51.9	51.6	73.1	85	83.3	81.2	84.5	81.5	84.7	88.1
Trace elements (ppm)																	
As	9.82	10.7	9.64	10.8	9.29	12.2	11.7	33.4	12.3	9.94	10.6	11.5	11.1	12.3	12.7	13.1	7.67
Sc	0.51	0.39	0.35	0.40	0.38	0.3	0.40	0.33	0.48	0.31	0.28	0.35	0.34	0.35	0.4	0.45	0.48
V	135	43.3	10.9	5.7	bdl	6.9	25	4.5	2.2	13	25	22	31	29	33	56	31
Cr	150	15	7	9	2	13	68	5	11	10	172	134	156	182	253	311	363
Co	1035	1003	812	769	946	495	890	408	385	703	1001	1048	1001	972	990	1080	1266
Rb	0.16	0.11	0.06	0.06	0.07	0.08	0.05	0.05	0.03	0.05	0.09	0.05	0.05	0.03	0.04	0.05	bdl
Sr	0.98	0.6	0.33	0.51	0.49	0.92	0.35	0.49	0.47	0.34	0.53	0.43	0.57	0.37	0.34	0.42	0.40
Ba	2.7	3.6	0.7	6.8	2.4	1.8	1.9	2.3	2.5	6.5	4.4	1.2	1.8	2.0	2.4	1.4	1.4
Y	0.04	0.07	0.08	0.08	0.05	0.59	0.03	0.22	0.18	0.07	0.02	0.03	0.07	0.02	0.04	0.09	bdl
Zr	2.7	1.5	1.4	1.1	0.34	0.79	0.45	0.55	0.49	0.72	0.40	0.29	0.53	0.35	0.30	0.49	0.30
Hf	0.13	0.04	0.02	0.08	0.02	0.02	0.06	0.03	0.04	0.03	0.02	0.02	0.03	0.03	0.04	0.06	0.02
Nb	0.84	1.1	1.5	1.2	0.11	0.90	0.15	0.73	0.81	0.5	0.12	0.15	0.2	0.17	0.13	0.31	0.06
Ta	0.03	0.02	0.02	0.02	0.01	0.02	0.01	0.01	0.02	0.01	0.01	0.01	0.01	0.01	0.01	0.01	0.01
Th	0.02	0.03	0.03	0.06	0.04	0.17	0.05	0.07	0.06	0.05	0.02	0.02	0.04	0.01	0.02	0.04	0.01
U	0.03	0.03	0.06	0.09	0.11	0.18	0.09	0.19	0.17	0.11	0.06	0.05	0.07	0.04	0.05	0.04	0.01
La	0.03	0.05	0.07	0.11	0.08	0.42	0.07	0.11	0.09	0.01	0.03	0.04	0.05	0.01	0.01	0.04	0.01
Ce	0.06	0.13	0.26	0.29	0.26	1.2	0.21	0.49	0.34	0.06	0.07	0.10	0.13	0.02	0.03	0.10	0.03
Pr	0.01	0.02	0.02	0.04	0.03	0.15	0.02	0.04	0.04	bdl	0.01	0.01	0.01	bdl	bdl	0.01	bdl
Nd	0.03	0.07	0.09	0.15	0.11	0.72	0.09	0.20	0.17	0.02	0.02	0.04	0.06	0.01	0.01	0.04	0.01
Sm	0.01	0.02	0.02	0.04	0.03	0.2	0.02	0.06	0.06	0.01	0.01	0.01	0.01	bdl	bdl	0.01	bdl
Eu	bdl	0.01	0.01	0.01	bdl	0.04	0.01	0.01	0.01	bdl	bdl	bdl	bdl	bdl	bdl	bdl	bdl
Gd	0.01	0.02	0.21	0.03	0.02	0.18	0.01	0.06	0.05	0.01	bdl	0.01	0.01	bdl	bdl	0.01	bdl
Tb	bdl	bdl	0.07	0.01	bdl	0.03	bdl	0.01	0.01	bdl	bdl	bdl	bdl	bdl	bdl	bdl	bdl
Dy	0.01	0.02	0.02	0.03	0.01	0.18	0.01	0.08	0.08	0.01	bdl	0.01	0.01	bdl	bdl	0.01	bdl

Table 1 (continued)

Sample No.	BMZ-90	BMZ-91	BMZ-92	BMZ-93	BMZ-94	BMZ-95	BMZ-96	BMZ-97	BMZ-98	BMZ-99	BMZ-100	BMZ-101	BMZ-102	BMZ-103	BMZ-104	BMZ-105	BMZ-106
Ho	bdl	bdl	bdl	0.01	bdl	0.03	bdl	0.01	0.01	bdl	bdl	bdl	bdl	bdl	bdl	bdl	bdl
Er	bdl	0.01	0.01	0.01	0.01	0.07	bdl	0.03	0.03	bdl	bdl	bdl	0.01	bdl	bdl	0.01	bdl
Tm	bdl	bdl	bdl	bdl	bdl	0.01	bdl	bdl	bdl	bdl	bdl	bdl	bdl	bdl	bdl	bdl	bdl
Yb	bdl	0.01	0.01	0.01	bdl	0.04	bdl	0.02	0.02	bdl	bdl	bdl	bdl	bdl	bdl	bdl	bdl
Lu	bdl	bdl	bdl	bdl	bdl	bdl	bdl	bdl	bdl	bdl	bdl	bdl	bdl	bdl	bdl	bdl	bdl
Platinum-group elements (ppb)																	
Ir	2.12	1.84	1.19	0.93	0.81	0.59	0.83	0.59	0.62	0.86	1.26	1.2	1.1	1.12	1.1	1.72	5.61
Ru	1.29	1.34	1	0.89	0.78	0.61	0.91	0.59	0.53	0.86	1.21	1.46	0.93	1.44	1.01	1.48	8.06
Rh	0.75	0.43	0.31	0.19	0.3	0.29	0.18	0.08	0.21	0.43	0.2	0.39	0.53	0.43	0.27	0.76	0.96
Pt	48.8	59.6	87.5	195	148	210	167	180	222	162	103	104	130	159	163	71.1	32.3
Pd	59.4	154	140	157	130	313	159	302	249	223	123	78	141	156	130	91.8	37.8

bdl: below detection limit

solid solution (MSS) (Fig. 3b). The exsolution of pentlandite from pyrrhotite (Fig. 3a,c) indicates that both minerals originally crystallized as MSS from the sulfide melt between 1,100 and 800°C (Naldrett 1969; Craig and Scott 1973).

Cobaltite–gersdorffite solid solution in the massive ores shows well-developed compositional zoning of Co and Ni parallel or sub-parallel to the crystal faces on the X-ray scanning images (not shown in this paper), and is unaltered in early formed zones. Continuous compositional variations in the CGSS indicate gradual changes related to progressive crystallization. These features indicate that the CGSS is also magmatic in origin and crystallized from the sulfide melt. Similar compositional zoning in CGSS was described from the Las Aguilas Ni–Cu deposits in Argentina (Gervilla et al. 1997; Fernando et al. 1997), from the Mount General'skaya layered intrusion in Russia (Barkov et al. 1999), and from the Yangliuping sulfide deposit in SW China (Song et al. 2004) where the CGSS is interpreted to have crystallized from an As-bearing residual sulfide liquid (Hakli et al. 1976).

The Pd/Ir ratio is a good indicator of the origin of sulfide ores. Magmatic sulfide ores have relatively low Pd/Ir ratios, whereas hydrothermal sulfide ores have very high Pd/Ir ratios (Keays et al. 1982; Keays 1995) because Pd and Ir are fractionated during alteration (Barnes et al. 1985). Iridium is not easily leached from the source rocks or readily transported by fluids. Hydrothermal sulfides thus have extremely low Ir contents, resulting in high Pd/Ir ratios (Keays et al. 1982). The massive ores in Baimazhai have highly variable Pd/Ir ratios ranging from 6.7 to 530, probably indicating variable degrees of hydrothermal alteration. The low Ir contents (<2 ppb) and high Pd/Ir ratios (>80) of the samples can be interpreted to have been modified by hydrothermal activities, whereas a few samples with relatively high Ir contents (2.1 to 5.6) and low Pd/Ir ratios (6.7 to 28) are considered to be a magmatic feature. Most of the massive ores plot approximately along the mantle line and have a trend from Ni-rich to Cu-rich sulfide melt in the Ni/Cu vs Pd/Ir plot (Fig. 6). The lowest Pd/Ir ratio (6.7) for the massive ores is similar to the average ratio (6.26) of komatiites in Kambalda, which have the lowest and most 'primitive' Pd/Ir ratios of any terrestrial magmatic liquid (Keays 1982). Therefore, relatively high Ir contents and highly variable Pd/Ir ratios of the massive ores in Baimazhai indicate that the sulfides originally formed by magmatic processes but were later modified by hydrothermal alteration.

Typically, alteration of primary Ni–Cu sulfides results in the formation of Cu-rich ores, accompanied by mineral phases such as Pt-rich and Pd-rich arsenides, tellurides and Bi-bearing minerals (Watkinson and Melling 1992; Farrow and Watkinson 1999). Such modified ores tend to be enriched in

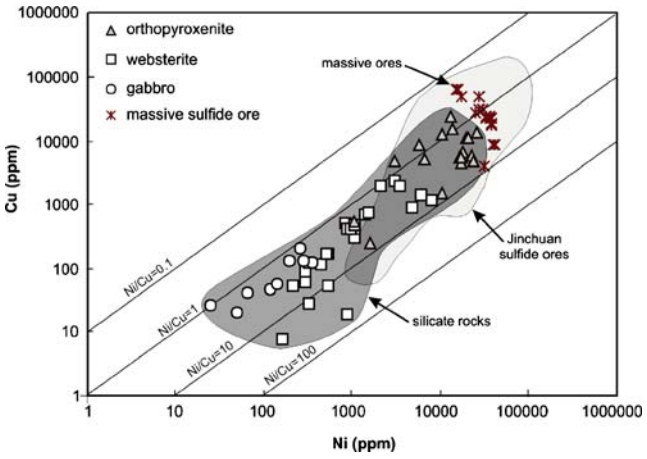

Fig. 4 Cu vs Ni plot of the Baimazhai massive ores in comparison with the Baimazhai silicate rocks and the Jinchuan sulfide ores. Data source: Baimazhai silicate rock from Wang et al. (2006); Jinchuan sulfide ores from Chai and Naldrett (1992b)

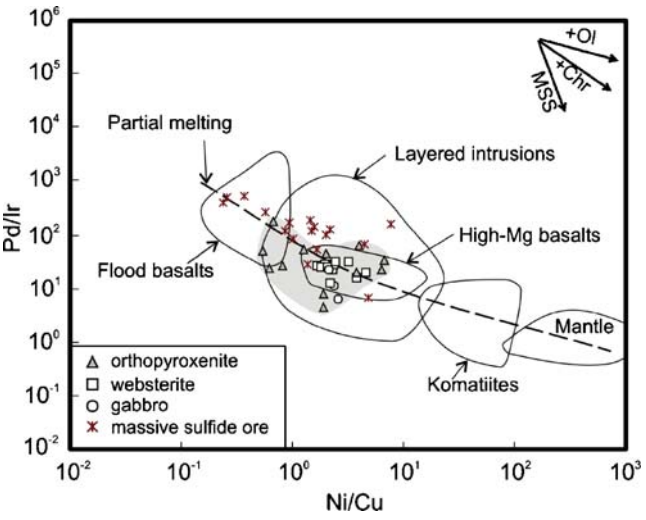

Fig. 6 Ni/Cu vs Pd/Ir diagram of the Baimazhai massive ores in comparison with the Baimazhai silicate rocks. Reference fields are after Barnes et al. (1988)

Cu, Au and Pd. Therefore, at Baimazhai, the samples with high Pd/Ir ratios usually have low Ni/Cu ratios (Fig. 6). Hydrothermal alteration in the Baimazhai deposit is also revealed by the presence of bismuthide and telluride phases, rather than primary Po–Pn–Cp assemblages, such as native bismuth, parkerite and hedleyite. The melting point of pure Bi is very low (271.4°C), and thus, it must form during a low-temperature post-magmatic hydrothermal stage.

The froodite in Baimazhai is likely hydrothermal in origin because it is associated with native bismuth. It may have formed by the interaction of hydrothermal fluids with earlier primary magmatic sulfides such that PGE are remobilized and re-precipitated to form PGM. Because Pd

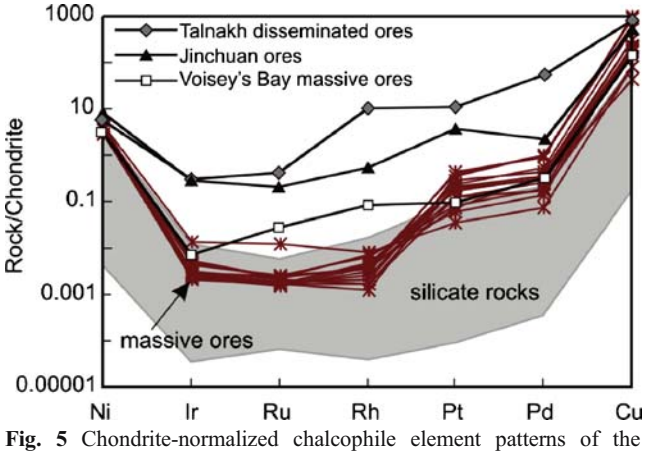

Fig. 5 Chondrite-normalized chalcophile element patterns of the Baimazhai massive ores in comparison with the Baimazhai silicate rocks and the ores of some other deposits related to mafic intrusions (Voisey's Bay, Talnakh and Jinchuan). Normalization values are from Anders and Grevesse (1989). Ore compositions are recalculated to 100% sulfide. Data sources: Baimazhai from Wang et al. (2006), Voisey's Bay from Naldrett (2004), Talnakh from Naldrett et al. (2000), and Jinchuan from Chai and Naldrett (1992b)

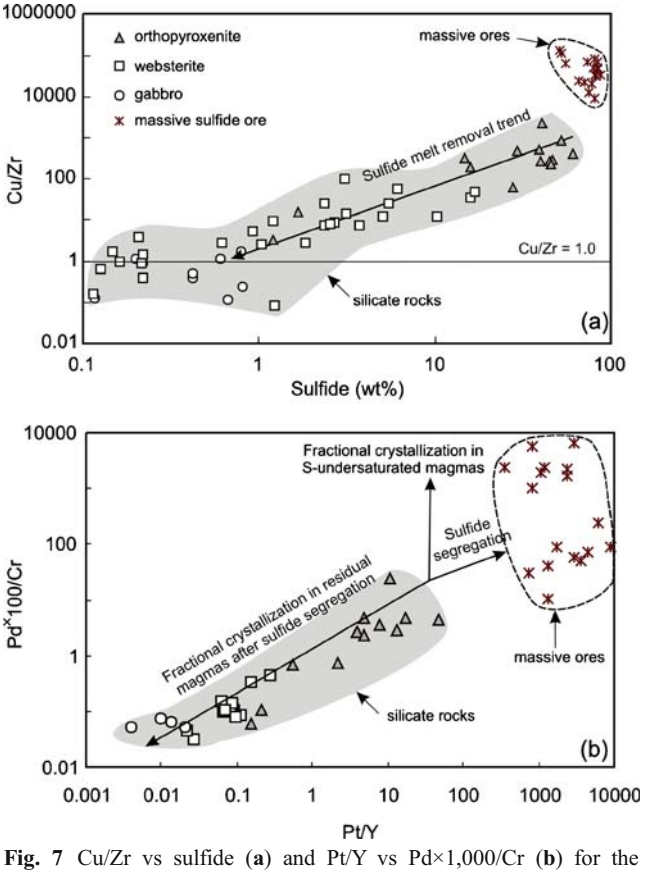

Fig. 7 Cu/Zr vs sulfide (**a**) and Pt/Y vs Pd×1,000/Cr (**b**) for the Baimazhai massive ores in comparison with the Baimazhai silicate rocks

is more mobile than the other PGE, froodite is a common PGM in the hydrothermal veins of many sulfide deposits, such as those in Sudbury (Molnár et al. 2001).

R-factor and excess sulfides of the Baimazhai intrusion

Calculation of the *R*-factor, the ratio of the volume of silicate melt to the volume of sulfide melt from which the ore formed, is based on the compositions of sulfide ores and silicate magmas from which the sulfide melts segregated. The following equation (Campbell and Naldrett 1979) is used to estimate the *R*-factor:

$$\mathrm{Cs} = \mathrm{Co} \times D \times (R+1)/(R+D)$$

in which Cs=the concentration of a trace element in the sulfide liquid, Co=the initial concentration of that trace element in the silicate liquid, and *D*=the distribution coefficient for the partitioning of the trace element between the sulfide and silicate liquids.

The massive ores of Baimazhai have Ni/Cu ratios similar to those of the Jinchuan deposit (Ni/Cu=0.2 to 18 with an average of 4.8) (Fig. 4), which are believed to have formed from a high-Mg basaltic magma with ~12 wt% MgO (Chai and Naldrett 1992a). The massive ores have chondrite-normalized chalcophile element patterns comparable to the ores of the Voisey's Bay, Noril'sk-Talnakh and Jinchuan deposits that are associated with igneous bodies formed from basaltic or MgO-rich basaltic magmas (Naldrett and Duke 1980) (Fig. 5), suggesting that the Baimazhai massive ores also formed from Mg-rich basaltic magmas, comparable to the parental, siliceous high-magnesium basaltic magmas invoked for the Baimazhai intrusion (Wang et al. 2006). The siliceous, high-magnesium basaltic magmas are thought to have formed from low-Ti Emeishan picritic parental magmas by extensive crustal contamination (~35%) (Wang et al. 2006).

The average Ni content in 100% massive sulfides is 4.1 wt%. Given that the Emeishan picritic magma contained an average of 18.7 wt% MgO (=735 ppm Ni, after Wang et al. 2006, Table 1) and a partition coefficient $D_{\mathrm{sul/sil}}$ of 250 for Ni, we obtain an *R*-factor of ~70 for the Baimazhai sulfides. Clearly, the 18.7 wt% MgO (=735 ppm Ni) is only an estimate of the composition, and the *R*-factor would differ significantly if either the Ni content of the magmas or the partition coefficient varied. However, the *R*-factor estimated for the Baimazhai ores is much lower than that calculated for the Noril'sk-Talnakh ores (10,000–100,000) (Brügmann et al. 1993). The Baimazhai intrusion has PGE tenors that are 20 to 120 times lower than those of the giant Noril'sk-Talnakh deposit in Russia. The low *R*-factor of the Baimazhai deposit thus accounts for the low PGE concentrations and the paucity of PGM in the massive ores.

The solubility of S in the parental magma of the Baimazhai intrusion can be estimated from the following equation (Li and Ripley 2005):

$$\begin{aligned} \ln Xs = {} & 1.229 - 0.74\left(10^4/T\right) - 0.021(P) - 0.311 \ln X_{FeO} \\ & - 6.166X_{SiO2} - 9.153X_{Na2O+K2O} - 1.914X_{MgO} \\ & + 6.594X_{FeO} \end{aligned}$$

$$Moles\ S = (Xs) \times (moles\ oxides\ in\ magma)/(1 - Xs)$$

Again, the parental magma of the intrusion is assumed to be similar to that of the Emeishan picritic magma (c.f. Wang et al. 2006), which had an average composition of 10.7 wt% FeO (=0.091 mol%), 18.7 wt% MgO (=0.285 mol%), 43.7 wt% SiO_2 (=0.446 mol%), 0.94 wt% Na_2O (=0.009 mol%) and 0.12 wt% K_2O (=0.0008 mol%) (data after Table 1 of Wang et al. 2006). Using this composition, the predicted ln *X*s at a pressure of 1 kbar and 1200°C is −5.86, corresponding to 0.1497 wt% S, equivalent to 0.39 wt% sulfide in the parental magma. However, at least 70% of the intrusion is mineralized with an average of 54 wt% sulfide in the net-textured and massive ores. Hence, the Baimazhai intrusion contains a much higher quantity of sulfides than its parental magma would have been able to dissolve.

Sulfide removal and accumulation in a staging magma chamber

At Baimazhai, the sulfide-poor gabbros and websterites with low Cu/Zr ratios (<1) are believed to have formed from magmas that had already undergone sulfide segregation, and Cu that was removed by this process was concentrated in the massive ores (Cu/Zr=8,700 to 133,000) and in the ortho-pyroxenites (Cu/Zr=3.3 to 2,240) (Fig. 7a). Chromium is a compatible element that is removed from magmas by early crystallized minerals (e.g. olivine and chromite) and decreases during fractional crystallization of S-undersaturated magmas, whereas Pd is highly incompatible under these conditions (Keays 1995) and Pt is moderately compatible in chromite (Peck and Keays 1990). Therefore, under S-undersaturated conditions, Pd/Cr ratios will increase with the fractionation of magmas, whereas Pt/Y ratios will either remain constant (if chromite is not a fractionating phase) or decrease slightly because Y is strongly incompatible. However, Pt and Pd have extremely high sulfide/silicate liquid partition coefficients on the order of 10^3 to 10^5, much higher than those of Ni or Cu (Bezmen et al. 1994), such that Pt and Pd can be efficiently extracted from magmas by minute amounts of segregating sulfide droplets. If segregation of immiscible sulfide melts occurs,

Pd/Cr and Pt/Y ratios will then dramatically decrease in the residual magmas. At Baimazhai, the gabbros with low Pd/Cr and Pt/Y ratios may represent the residual magmas after the segregation of immiscible sulfide melts, which subsequently formed the massive ores with high Pd/Cr and Pt/Y ratios (Fig. 7b).

The massive ores at Baimazhai have Ni/Cu, Pd/Pt and Cu/Pd ratios similar to those of the silicate rocks of the intrusion [Ni/Cu=0.5 to 6.7, Pd/Pt=0.7 to 3.5 and Cu/(Pd×1,000)=100 to 400] (Wang et al. 2006). They also have chondrite-normalized chalcophile element patterns comparable to those of the silicate rocks (Fig. 5). These similarities indicate that the sulfides of the Baimazhai massive ores are co-genetic with those of the silicate rocks. The Pd/Pt ratio of the massive ores averages 1.2, much lower than those for Noril'sk (3 to 5) (Lightfoot and Keays 2005), indicating that all sulfides in Baimazhai formed in a single sulfide saturation event (c.f. Lightfoot and Keays 2005). In the Noril'sk body, high metal tenors of the sulfides were upgraded as the staging chamber was replenished by new batches of primitive, chalcophile metal-enriched magma (Brügmann et al. 1993; Lightfoot and Keays 2005).

However, excess sulfides in Baimazhai must have been derived from a much larger volume of magma than the intrusion itself. Neither low *R*-factor (~70) nor extensive crustal contamination can be reached after emplacement to form the mineralized intrusion. Thus, for the Baimazhai deposit, we propose that a large staging magma chamber developed in the upper crust, and that the immiscible sulfides settled toward the base of the chamber. This stratified magma chamber eventually had sulfide-free magma at its top and sulfide-laden magma at its base.

Disposition of sulfides in the Baimazhai intrusion

Mineralized intrusions with excess sulfides may be formed by the continuous flow of magma through a dynamic magma conduit (see Lesher and Keays 2002) or by flow differentiation in a dynamic magma conduit (Barker 1983).

Elsewhere within the ELIP, the Yangliuping sulfide deposit and the Jinbaoshan Pd–Pt deposit have sulfide ores concentrated in the lower parts of differentiated sills (Song et al. 2003; Wang et al. 2005). Like those in the Noril'sk region, these deposits are considered to have formed in magma conduits through which large volumes of silicate magma passed and left behind sulfide droplets together with early crystallized silicate minerals, such as olivine (Naldrett and Lightfoot 1999).

The distribution of both sulfides and Opx cumulates in the Baimazhai intrusion is radically different from the other deposits in the ELIP, but the body may have formed in a similar manner. The concentration of massive sulfides in the central part of the intrusion can be explained by flow differentiation in a dynamic magma conduit, a common phenomenon in igneous petrology. Ross (1986) attributed the distribution of plagioclase phenocrysts across a 5.6-m-thick porphyritic, alkaline dolerite dyke in Rockport, MA, to flow differentiation, where the phenocryst concentrations in the dyke increase from nearly zero at its margins to 46 vol.% at its center. Li et al. (2004) and de Waal et al. (2004) proposed a model to explain the concentration of sulfide by the emplacement of sulfide-bearing crystal mush along a planar fracture for the Jinchuan intrusion in NW China. Although the Jinchuan intrusion occurs along planar fractures, the distribution of its sulfide deposits in the central part of the intrusion is geometrically similar to the Baimazhai deposit. The presence of the sulfide ore body in the center of the Baimazhai intrusion and the distribution of net-textured and massive sulfide ores are also similar to that of the Hongqiling deposit in NE China (Zhou et al. 2002a).

The Baimazhai deposit probably formed in a convergent setting as the deposit occurs along what was the boundary between the Indochina and Yangtze Blocks (Fig. 1a) in the Permian (Yan et al. 2006). Compressive stresses associated with the convergent boundary evacuated the staging chamber from the top downwards and emplaced the intrusion in the overlying Ordovician strata. The Baimazhai intrusion is interpreted as a conduit through which both silicate melt and sulfide liquid passed. The migrating magma underwent flow differentiation due to the higher velocity of the magma in the centre of the conduit. Because the sulfide melts were denser than the silicate melt, the sulfide melts were more or less centrally disposed in the flowing magma. As a consequence, sulfides were concentrated at the centre of the intrusion and decreased more or less systematically towards the margin of the intrusion.

Conclusions

The Baimazhai deposit contains a massive sulfide ore body centrally disposed in the host mafic–ultramafic intrusion. The similar Pd/Pt and Cu/Pd ratios between the massive ores and the silicate rocks of the intrusion indicate a single sulfide segregation event. The deposit is magmatic in origin but was strongly overprinted by hydrothermal activity. It is suggested that the Baimazhai deposit was formed by flow differentiation when immiscible sulfide melts and silicate liquids in a deep-seated staging magma chamber migrated upward along a magma conduit. The heavy sulfide melts were concentrated in the central part of the conduit to form a massive sulfide ore body. Excess sulfides in the intrusion and low *R*-factor accounts for the low PGE concentrations and rare PGMs in the massive ores.

Acknowledgements This study was substantially supported by research grants from the Research Council of Hong Kong, China (HKU 7056/03P and HKU 7057/05P), an outstanding young researcher award to MFZ from the Nature Science Fund of China (40129001) and a CRCG grant from the University of Hong Kong. The Jinping Nickel Mine is thanked for the assistance with the field work and the collection of drill core samples. Valuable contributions are acknowledged from Prof. Reid R. Keays and Dr. Chusi Li. We thank Mr. L. Qi, and Ms. Y. Liu for the help with the sample analyses. Prof. P.T. Robinson is gratefully acknowledged for reading an early draft of this manuscript. We thank Dr. Louis J. Cabri, Dr. X.Y. Song and Dr. P. Lightfoot for their critical comments, which helped to improve the manuscript.

References

Anders E, Grevesse N (1989) Abundances of the elements: meteoritic and solar. Geochim Cosmochim Acta 53:197–214

Barker DS (1983) Igneous rocks. Prentice Hall, New Jersey, pp132–133

Barkov AY, Thibault Y, Laajoki KVO, Melezhik VA, Nilsson LP (1999) Zoning and substitutions in Co–Ni–(Fe)–PGE sulfarsenides from the Mount General'skaya layered intrusion, Arctic Russia. Can Mineral 37:127–142

Barnes S-J, Naldrett AJ, Gorton MP (1985) The origin of the fractionation of platinum-group elements in terrestrial magmas. Chem Geol 53:303–323

Barnes S-J, Kornelliussen BR, Nilssen A, Often L-P, Pedersen R-B, Robins B (1988) The use of mantle normalization and metal ratios in discriminating the effects of partial melting, crystal fractionation and sulphide segregation on platinum group elements, gold, nickel and copper: examples from Norway. In: Prichard HM, Potts PJ, Bowles JFW, Cribb SJ (eds) Geo-platinum 87. Elsevier, London, pp113–143

Bezmen NS, Asif M, Brügmann GE, Romamekno IM, Naldrett AJ (1994) Experimental determinations of sulphide–silicate partitioning of PGE and Au. Geochim Cosmochim Acta 58:1251–1260

Brügmann GE, Naldrett AJ, Asif M, Lightfoot PC, Gorbachev NS, Fedorenko VA (1993) Siderophile and chalcophile metals as tracers of the evolution of the Siberian trap in the Noril'sk region, Russia. Geochim Cosmochim Acta 57:2001–2018

Campbell IH, Naldrett AJ (1979) The influence of silicate:sulphide ratios on the geochemistry of magmatic sulfides. Econ Geol 74:1503–1505

Chai G, Naldrett AJ (1992a) The Jinchuan ultramafic intrusion: cumulate of a high-Mg basaltic magma. J Petrol 33:277–303

Chai G, Naldrett AJ (1992b) Characteristics of Ni–Cu–PGE mineralisation and genesis of the Jinchuan deposit, Northwest China. Econ Geol 87:1475–1495

Chung SL, Jahn BM (1995) Plume–lithosphere interaction in generation of the Emeishan flood basalts at the Permian–Triassic boundary. Geology 23:889–892

Craig JR, Scott SD (1973) Pentlandite–pyrrhotite and other low temperature relations in the Fe–Ni–S systems. Am J Sci 273A:496–910

de Waal SA, Xu Z, Li C, Mouri H (2004) Emplacement of viscous crystal mushes: Jinchuan ultramafic intrusion, Western China. Can Mineral 42:371–392

Farrow CEG, Watkinson DH (1999) An evaluation of the role of fluids in NI–Cu–PGE-bearing, mafic–ultramafic systems. In: Keays RR, Lesher CM, Lightfoot PC, Farrow CEG (eds) Dynamic processes in magmatic ore deposits and their application in mineral exploration. Geol Assoc Can Short Course Notes 13: 31–67

Fernando G, Alejandro SA, Rogelio DA, Purificacion FHA, Andres P (1997) Platinum-group element sulpharsenides and Pd bismuthotellurides in the metamorphosed Ni–Cu deposit at Las Aguilas (province of San Luis, Argentina). Mineral Mag 61:861–877

Gauert CDK, de Waal SA, Wallmach T (1995) Geology of the ultrabasic to basic Uitkomst complex, eastern Transvaal, South Africa: an overview. J Afr Earth Sci 21:553–570

Gervilla F, Sanchez-Anguita A, Acevedo RD, Fenoll Hach-Ali P, Paniagua A (1997) Platinum-group element sulpharsenides and Pd bismuthotellurides in the metamorphosed Ni–Cu deposit at Las Aguilas (Province of San Luis, Argentina). Mineral Mag 61:861–877

Guan T, Huang ZL, Xie LH, Xu C, Li WB (2003) Geochemistry of lamprophyres in Baimazhai nickel deposit, Yunnan Province: major and trace elements. Acta Mineralogica Sinica 23:278–288 (in Chinese with English abstract)

Hakli TA, Hanninen E, Vuorelaimen Y, Papunen H (1976) Platinum-group minerals in the Hitura nickel deposit, Finland. Econ Geol 71:1206–1213

Keays RR (1982) Palladium and iridium in komatiites and associated rocks: application to petrogenetic problems. In: Arndt NT, Nisbet EG (eds) Komatiites. George Allen & Unwin, London, pp 435–455

Keays RR (1995) The role of komatiitic and picritic magmatism and S-saturation in the formation of the ore deposits. Lithos 34:1–18

Keays RR, Nickel EH, Groves DI, McGoldrick PJ (1982) Iridium and palladium as discriminants of volcanic-exhalative, hydrothermal, and magmatic nickel sulfide mineralization. Econ Geol 77:1535–1547

Kelly DP, Vaughan DJ (1983) Pyrrhotite–pentlandite ore textures: a mechanistic approach. Mineral Mag 47:457–463

Lesher CM, Keays RR (2002) Komatiite-associated Ni–Cu–(PGE) deposits. In: Cabri LJ (ed) The geology, geochemistry, mineralogy, mineral beneficiation of the platinum-group elements. Canadian Institute of Mining, Metallurgy and Petroleum, Special Volume 54:579–618

Li C, Ripley EM (2005) Empirical equations to predict the sulfur content of mafic magmas at sulfide saturation and applications to magmatic sulfide deposits. Miner Depos 40:218–230

Li C, Xu Z, de Waal SA, Ripley EM, Maier WD (2004) Compositional variations of olivine from the Jinchuan Ni–Cu sulfide deposit, Western China: implications for ore genesis. Miner Depos 39: 159–172

Lightfoot PC, Keays RR (2005) Siderophile and chalcophile metal variations in flood basalts from the Siberian Trap, Noril'sk Region: implications for the origin of the Ni–Cu–PGE sulfide ores. Econ Geol 100:439–462

Lightfoot PC, Naldrett AJ (1999) Geological and geochemical relationships in the Voisey's Bay intrusion, Nain Plutonic Suite, Labrador, Canada. In: Keays RR, Lesher CM, Lightfoot PC, Farrow CEG (eds) Dynamic processes in magmatic ore deposits and their application in mineral exploration. Geol Assoc Can Short Course Notes 13:1–30

Maier WD, Li C, de Waal SA (2001) Why are there no major Ni–Cu sulfide deposits in large layered mafic–ultramafic intrusions? Can Mineral 39:547–556

Molnár F, Watkinson DH, Jones PC (2001) Multiple hydrothermal processes in footwall units of the North Range, Sudbury Igneous Complex, Canada, and implications for the genesis of vein-type Cu–Ni–PGE deposits. Econ Geol 96:1645–1670

Naldrett AJ (1969) A portion of the system Fe–S–O between 900°C and 1080°C and its application to sulfide ore magma. J Petrol 10:171–201

Naldrett AJ (2004) Magmatic sulfide deposit: geology, geochemistry and exploration. Springer, Heidelberg Berlin New York, pp137–277

Naldrett AJ, Duke JM (1980) Platinum metals in magmatic sulfide ores. Science 208:1417–1428

Naldrett AJ, Lightfoot PC (1999) Ni–Cu–PGE deposits of the Noril'sk region, Siberia; their formation in conduits for flood basalt volcanism. In: Keays RR, Lesher CM, Lightfoot PC, Farrow CEG (eds) Dynamic processes in magmatic ore deposits and their application in mineral exploration. Geol Assoc Can Short Course Notes 13:195–249

Naldrett AJ, Fedorenko VA, Asif M, Shushen L, Kunilov VE, Stekhin AI, Lightfoot PC, Gorbachev NS (1996) Controls on the composition of Ni–Cu sulfide deposits as illustrated by those at Noril'sk, Siberia. Econ Geol 91:751–773

Naldrett AJ, Asif M, Krstic S, Li C (2000) The composition of ore at the Voisey's Bay Ni–Cu sulfide deposit with special reference to platinum-group elements. Econ Geol 95:845–866

Peck DC, Keays RR (1990) Insights into the behaviour of precious metals in primitive, S-undersaturated magmas: evidence from the Heazlewood River complex, Tasmania. Can Mineral 28:553–577

Prichard HM, Hutchinson D, Fisher PC (2004) Petrology and crystallization history of multiphase sulfide droplets in a mafic dike from Uruguay: implications for the origin of Cu–Ni–PGE sulfide deposits. Econ Geol 99:365–376

Qi L, Hu J, Gregoire DC (2000) Determination of trace elements in granites by inductively coupled plasma mass spectrometry. Talanta 51:507–513

Qi L, Zhou M-F, Malpas J, Sun M (2005) Determination of rare earth elements and Y in ultramafic rocks by ICP-MS after preconcentration using $Fe(OH)_3$ and $Mg(OH)_2$ coprecipitation. Geostand Geoanal Res 29:131–141

Ross ME (1986) Flow differentiation, phenocryst alignment, and compositional trends within a dolerite dike at Rockport, Massachusetts. Geol Soc Am Bull 97:232–240

Song XY, Zhou M-F, Wang YL, Zhang CJ, Cao ZM, Li Y (2001) Geochemical constrains on the mantle source of the Upper Permian Emeishan continental flood basalts, SW China. Int Geol Rev 43:213–225

Song XY, Zhou M-F, Cao ZM, Sun M, Wang YL (2003) Ni–Cu–(PGE) magmatic sulfide deposits in the Yangliuping area, Permian Emeishan igneous province, SW China. Miner Depos 38:831–843

Song XY, Zhou M-F, Cao ZM (2004) Genetic relationships between base-metal sulfides and platinum-group minerals in the Yangliuping Ni–Cu–(PGE) sulfide deposit, southwestern China. Can Mineral 42:469–483

Song XY, Zhou M-F, Wang CY, Qi L, Zhang CJ (2006) Role of crustal contamination in the formation of the Jinchuan Ni–Cu–(PGE) sulfide deposit, NW China. Int Geol Rev (in press)

Tang ZL (1993) Genetic model of the Jinchuan nickel–copper deposit. In: Kirkham RV, Sinclair WD, Thorpe RI, Duke JM (eds) Mineral deposit modeling. Geol Assoc Can Special Publication 40:389–401

Tang ZL, Li WY (1995) Mineralisation model and geology of the Jinchuan Ni–Cu sulphide deposit bearing PGE. Geol Publ House, Beijing, pp 61–66

Tang ZL, Ren DJ, Xue ZR, Mu YK (1989) Nickel deposits of China. In: Mineral deposits of China. Geol Publ House, Beijing, pp207–270 (in Chinese)

Wang CY, Zhou M-F, Zhao DG (2005) Mineral chemistry of chromite from the Permian Jinbaoshan Pt–Pd–sulphide-bearing ultramafic intrusion in SW China with petrogenetic implications. Lithos 83:47–66

Wang CY, Zhou M-F, Keays RR (2006) Geochemical constraints on the origin of the Permian Baimazhai mafic–ultramafic intrusion. Contrib Mineral Petrol 152:309–321

Watkinson DH, Melling DR (1992) Hydrothermal origin of platinum-group mineralization in low-temperature copper sulfide-rich assemblages, Salt Chuk intrusion, Alaska. Econ Geol 87:175–184

Xu YG, Chung SL, Jahn BM, Wu GY (2001) Petrologic and geochemical constraints on the petrogenesis of Permian–Triassic Emeishan flood basalts in southwestern China. Lithos 58: 145–168

Yan DP, Zhou M-F, Song HL, Wang XW, Malpas J (2003) Origin and tectonic significance of a Mesozoic multi-layer over-thrust system within the Yangtze Block (South China). Tectonophysics 361:239–254

Yan DP, Zhou M-F, Wang CY, Xia B (2006) Structural and geochronological constraints on the tectonic evolution of the Dulong–Song Chay tectonic dome in Yunnan Province, SW China. J Asian Earth Sci (in press)

YBGMR (Yunnan Bureau of Geology and Mineral Resources) (1990) Regional Geology of Yunnan Province. Geological Memoirs, MGMR, S.1, N.21. Geol Publ House, Beijing, pp554 (in Chinese)

Zhang XS, Pirajno F, Qin DX, Fan ZG, Liu GL, Nian H (2006) Baimazhai, Yunnan Province, China: a hydrothermally modified magmatic nickel–copper–PGE sulfide deposit. Int Geol Rev 48:725–741

Zhou M-F, Yang ZX, Song XY, Lesher CM, Keays RR (2002a) Magmatic Ni–Cu–(PGE) sulfide deposits in China. In: Cabri LJ (ed) The geology, geochemistry, mineralogy, mineral beneficiation of the platinum-group elements. Canadian Institute of Mining, Metallurgy and Petroleum, Special Volume 54:619–636

Zhou M-F, Malpas J, Song XY, Kennedy AK, Robinson PT, Sun M, Lesher CM, Keays RR (2002b) A temporal link between the Emeishan large igneous province (SW China) and the end-Guadalupian mass extinction. Earth Planet Sci Lett 196:113–122